



Using Thoracic Ultrasonography to Accurately Assess Pneumothorax Progression During Positive Pressure Ventilation

A Comparison With CT Scanning

Nils Petter Oveland, MD; Hans Morten Lossius, MD, PhD; Kristian Wemmelund, cand med; Paal Johan Stokkeland, MD; Lars Knudsen, MD, PhD; and Erik Sloth, MD, PhD, DMSc

Background: Although thoracic ultrasonography accurately determines the size and extent of occult pneumothoraces (PTXs) in spontaneously breathing patients, there is uncertainty about patients receiving positive pressure ventilation. We compared the lung point (ie, the area where the collapsed lung still adheres to the inside of the chest wall) using the two modalities ultrasonography and CT scanning to determine whether ultrasonography can be used reliably to assess PTX progression in a positive-pressure-ventilated porcine model.

Methods: Air was introduced in incremental steps into five hemithoraces in three intubated porcine models. The lung point was identified on ultrasound imaging and referenced against the lateral limit of the intrapleural air space identified on the CT scans. The distance from the sternum to the lung point (S-LP) was measured on the CT scans and correlated to the insufflated air volume.

Results: The mean total difference between the 131 ultrasound and CT scan lung points was 6.8 mm (SD, 7.1 mm; range, 0.0-29.3 mm). A mixed-model regression analysis showed a linear relationship between the S-LP distances and the PTX volume ($P < .001$).

Conclusions: In an experimental porcine model, we found a linear relation between the PTX size and the lateral position of the lung point. The accuracy of thoracic ultrasonography for identifying the lung point (and, thus, the PTX extent) was comparable to that of CT imaging. These clinically relevant results suggest that ultrasonography may be safe and accurate in monitoring PTX progression during positive pressure ventilation. *CHEST 2013; 143(2):415-422*

Abbreviations: CXR = chest radiograph; PTX = pneumothorax; S-LP = sternum-lung point

Physical examination, including lung auscultation, is insufficient for diagnosing a pneumothorax (PTX) in blunt trauma victims.^{1,2} The most common adjunct

used to evaluate a PTX is the plain chest radiograph (CXR) but this modality has a low sensitivity for detecting intrapleural air in patients with trauma, who are typically confined in the supine position for spinal immobilization.^{3,4} As a consequence, more than

Manuscript received June 13, 2012; revision accepted July 23, 2012.

Affiliations: From the Department of Research and Development (Drs Oveland and Lossius), Norwegian Air Ambulance Foundation, Droebak, Norway; the Department of Anesthesiology and Intensive Care (Dr Oveland) and the Department of Radiology (Dr Stokkeland), Stavanger University Hospital, Stavanger, Norway; the Department of Surgical Sciences (Dr Lossius), University of Bergen, Bergen, Norway; the Faculty of Health Sciences (Drs Wemmelund and Sloth), Institute of Clinical Medicine, Aarhus University, Aarhus, Denmark; and the Department of Anesthesiology and Intensive Care (Drs Knudsen and Sloth), Aarhus University Hospital, Aarhus, Denmark.

Funding/Support: The authors have reported to *CHEST* that no funding was received for this study.

Correspondence to: Nils Petter Oveland, MD, Department of Research and Development, Norwegian Air Ambulance Foundation, Mailbox 94, 1441 Droebak, Norway; e-mail: nils.petter.oveland@norskluftambulanse.no

© 2013 American College of Chest Physicians. This is an Open Access article distributed under the terms of the Creative Commons Attribution-Noncommercial License (<http://creativecommons.org/licenses/by-nc/3.0/>), which permits unrestricted use, distribution, and reproduction in any medium, provided the original work is properly cited. Information for commercial entities is available online.

DOI: 10.1378/chest.12-1445

one-half of all traumatic PTXs are found only by a CT chest scan,⁵ which is the gold standard diagnostic test for a PTX.^{4,6} Clinically silent and radiographically undetected PTXs that are subsequently identified on CT scans are defined as occult PTXs.⁷⁻⁹ Once an occult PTX is identified, it must be decided whether to undertake tube thoracostomy or to simply observe the patient.¹⁰ Inserting a chest tube, which many believe is the only safe and appropriate PTX treatment,⁷ is associated with a 22% risk of major complications.¹¹ Observation without chest drainage, considered sufficient in spontaneously breathing patients,¹² carries a risk of PTX progression during positive pressure ventilation. Occult PTXs can evolve into tension PTXs,⁷ at which point diagnostic and treatment delays are highly lethal.¹³ Thus, a reliable, easy, and repeatable method for monitoring PTXs is needed. Ultrasonography meets all these requirements and can be performed in almost any clinical setting.¹⁴ The first international evidence-based set of recommendations for lung ultrasonography, published in March 2012,¹⁵ contains no expert consensus on how ultrasonography compares with CT scanning for assessing PTX extensions. Further research is necessary.¹⁵ We aimed to determine the accuracy of ultrasound imaging for delineating PTX extensions and to compare ultrasonography and CT scan assessment of PTX progression during positive pressure ventilation in mechanically ventilated pigs.

MATERIALS AND METHODS

This was a laboratory study of a PTX in a porcine model. Qualified and experienced animal caretaker personnel monitored the health of the animals during the study period. The experiments complied with the guidelines for animal experimental studies issued by the Danish Inspectorate for Animal Experimentation under the Danish Ministry of Justice, which also approved the study. The study adhered to the principles in the *Guide for the Care and Use of Laboratory Animals*.¹⁶

Animal Model

Three female Danish Landrace pigs (mean \pm SD body weight = 56.0 \pm 2.0 kg) were used (supplied from a local farm owned by Aarhus University). The animals were anesthetized with a combination of fentanyl, ketamine, and propofol; intubated; and positive pressure ventilated using a transport respirator (Oxylog 3000; Dräger) set to a tidal volume of 750 mL, a respiratory rate of 15 breaths/min, a positive end-expiratory pressure of 2 to 4 cm H₂O, and an FIO₂ of 30%. The end-tidal CO₂ level was kept within the normal range (4.0-6.5 kPa). All the animals were monitored by ECG, and their core temperatures, invasive arterial BPs, oxygen saturations, and end-tidal CO₂ levels were trended. In the radiology department, the animals were fixed in the supine position on a CT scan table. A three-way stopcock catheter (BD Connecta; Becton, Dickinson and Company) was inserted into the pleural space through a small thoracotomy at the intersection of the fifth to the seventh intercostal space and the anterior axillary line (Fig 1). The catheter was then anchored to the surrounding muscle and fascia. Bilateral (n = 2) and unilateral (n = 1) PTXs were induced by incrementally injecting and withdrawing air

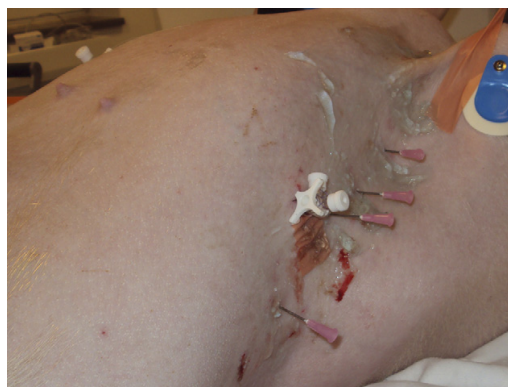


FIGURE 1. Chest of a porcine model with intrapleural catheter and needles.

from the pleural cavity using a 50-mL syringe (Omnifix, 50 mL; B. Braun Medical Inc) connected to the catheter. At the conclusion of the data collection, the animals were killed with an injection of pentobarbital.

Diagnostic Tests

Diagnostic ultrasound and CT scan thoracic evaluations were performed at 10 different PTX volumes. The PTX volumes were: 50, 100, 150, 200, 300, 400, 500, 600, 500, and 200 mL.

Ultrasonography: The ultrasound scans were performed by two experienced anesthesiologists using a Vivid Q ultrasound machine (General Electric Company) with a 12L-RS multifrequency 6-13 MHz linear array transducer (General Electric Company). To map the PTX topography, the pleural line between two ribs close to the sternum was identified. The probe was rotated to align with the intercostal space and was then gradually moved toward the lateral-inferior area of the chest. This maneuver was conducted to locate the point on the chest adjacent to the collapsed lung on the interior chest wall, which was defined as the “lung point.”¹⁷ The lung point corresponds to the lateral edge of the PTX.¹⁸ Subcutaneous needles that were easily visualized on the subsequent CT scan were placed during inspiration to designate the cutaneous projection of the lung points and the lateral limit of the intrapleural air collection. The number of needles used varied from two (for smaller PTXs) to four (for larger PTXs). The diagnostic algorithm for ultrasound identification of the lung point is illustrated in Figures 1 to 3.

CT Imaging: To define the extension of the intrapleural air collection, a non-contrast-enhanced CT scan was performed using a multislice CT scanner (Philips MX 8000 quad, Koninklijke Philips Electronics N.V.) with the following parameters: 120 kV, 120 to 150 mA, standard filter, 6.5-mm slice thickness, 3.2-mm slice increments, and a 310- to 360-mm field of view. A complete thoracic CT scan was obtained from the apex to the base during a short inspiratory hold period. The Digital Imaging and Communications in Medicine format pictures were stored and transferred to an archiving workstation. To optimize intrapleural air detection, the window width was adjusted to 1,500 Hounsfield units and the window level to -500 Hounsfield units.

Data Analysis

The accuracy of the ultrasound imaging for delineating the PTX extension was determined by measuring the distance from

Sonographic signs of pneumothorax (PTX)

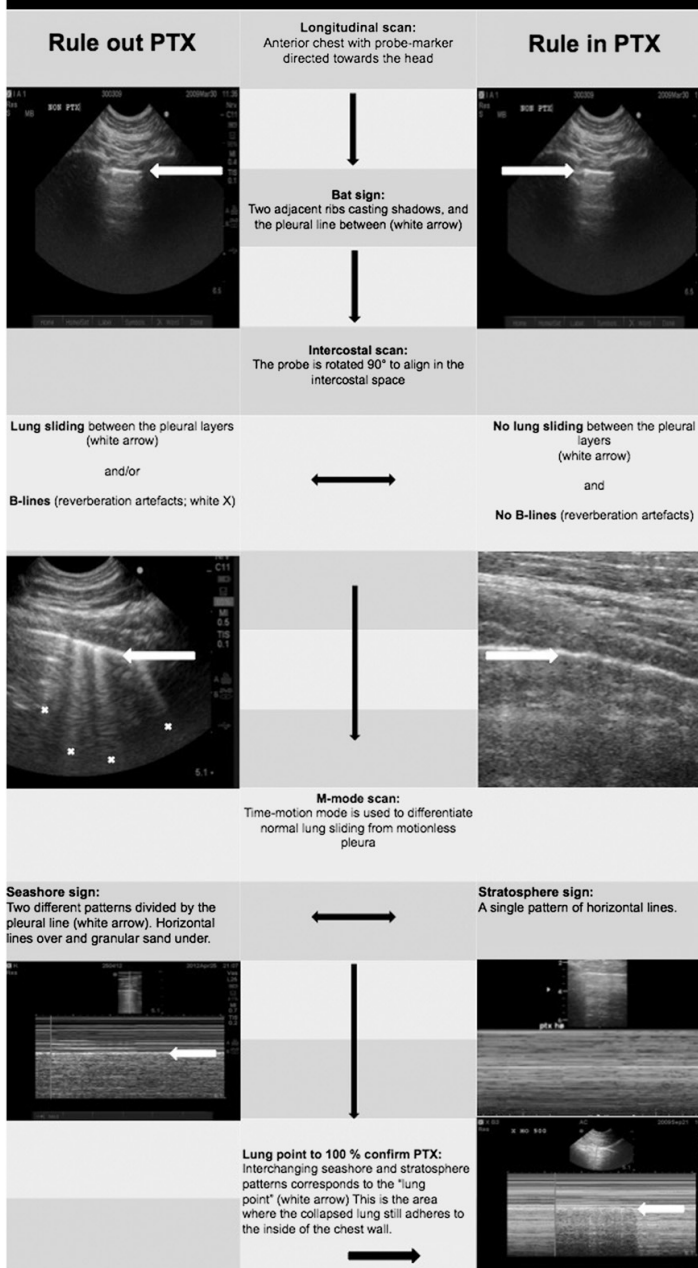


FIGURE 2. Flowchart suggesting the correct sequence for ultrasound identification of the lung point. The lung point is localized at the interface between two distinct sonographic patterns that are synchronous with respiration: one with no lung sliding (the "stratosphere sign" in M-mode) and the other with normal lung sliding (the "seashore sign" in M-mode) illustrated in the lower right corner. Demonstration of normal lung sliding is only possible on video clips.

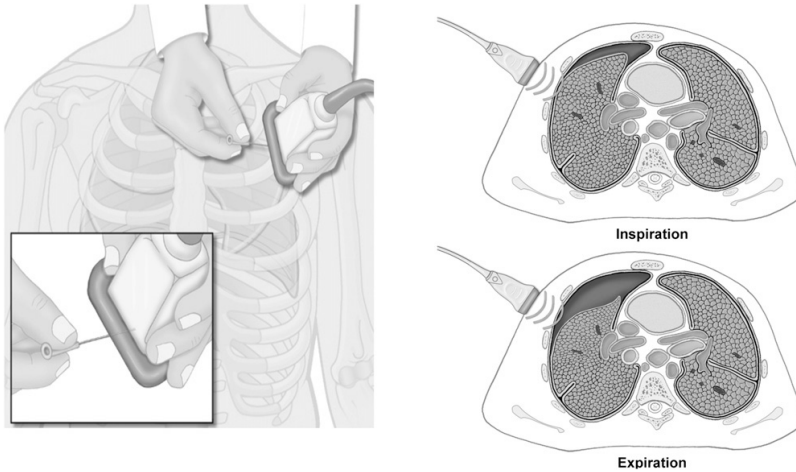


FIGURE 3. Lung points were located at the chest adjacent to the collapsed lung on the interior chest wall and aligned in the center of the ultrasound probe during inspiration. Needles were inserted to mark its cutaneous projection on the chest wall. (Illustrations: Kari M. Toverud [certified medical illustrator].)

the cutaneous needle tip to the lateral limit of the intrapleural air layer on the CT scan (Fig 4A). The difference in the lung point designations (Δ LP ultrasound-CT scan) was measured at three areas on the chest (the anterior chest between costae 1 and 5, the lateral chest between costae 5 and 8, and the posterior chest between costae 8 and 12), and the measurements were expressed as absolute and mean values (millimeters) with SDs and ranges. To reduce possible sources of bias, two readers performed all the measurements in random order, and the degree of agreement between their separate readings was analyzed using a Bland-Altman plot. A straight line from the central part of the sternum to the lung point (the S-LP distance) at two preset chest levels on the CT scans (the high level between costae 2 and 3 and the medium level between costae 5 and 6) was drawn to evaluate the

relation between lung point location and PTX size (Fig 4B). A mixed linear model regression was used to analyze the effects of PTX volume, increasing/decreasing PTX size, thoracic laterality, and chest levels on the S-LP distance. The interdependencies between the measurements in the porcine model were modeled by a compound (or autoregressive) correlation structure.¹⁹ All the statistical calculations were performed using SPSS 18.0 (IBM).

RESULTS

A total of 131 lung points were identified. The overall mean difference between the two modalities

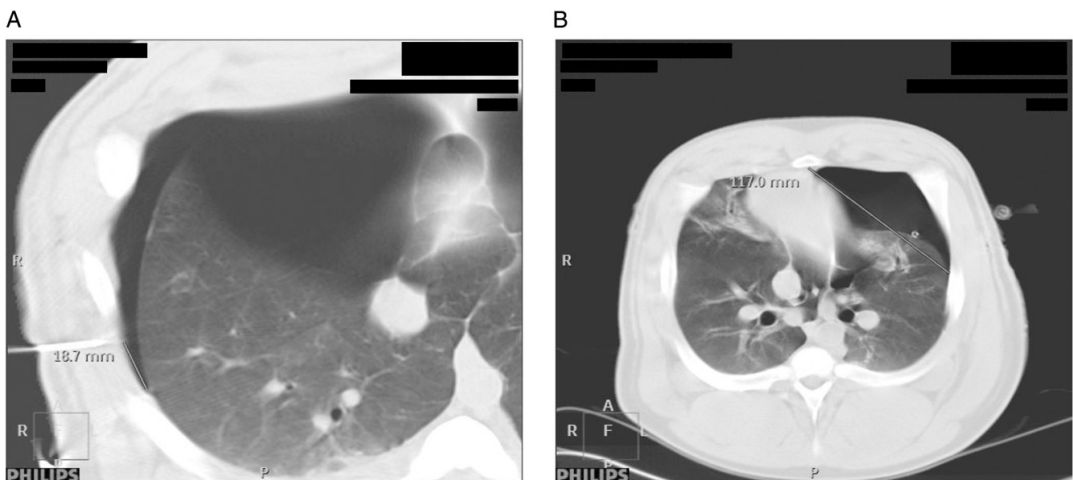


FIGURE 4. A, Difference in lung point localization was determined by comparing the ultrasound-placed needles with the extension of the PTX on the CT scans. B, The sternum-lung point (S-LP) distance. The lung is increasingly separated from the chest wall as the PTX expands, leading to lateralization of the lung point and increased S-LP distance. See Figure 2 legend for expansion of other abbreviations.

ultrasonography and CT imaging was 6.8 ± 7.1 mm, with colocation in the anterior, lateral, and posterior chest regions of 6.8 ± 8.6 mm, 6.4 ± 6.1 mm, and 7.3 ± 6.4 mm, respectively. The mean variance between the ultrasound and CT scan measurements of the lateral PTX limits was 0.0 to 29.3 mm (Table 1). Furthermore, there was a high level of agreement in the lung point measurements between readers one and two, as illustrated in the Bland-Altman plot (Fig 5). The 95% limits of agreement interval was -12.0 to 13.9 .²⁰

The mixed-model regression analysis revealed a linear relationship between the S-LP distance and the PTX volume ($P < .001$). The strength of the relation between the S-LP distance and the PTX volume differed between the left and right lungs ($P = .001$), but this divergence decreased at larger PTX volumes (Fig 6). When the PTX volume increased by 100 mL, the mean S-LP distance increased by 4 mm ($P < .001$) in the right lung and by 11 mm in the left ($P < .001$) (95% CIs, 0.01-0.07 and 0.08-0.13,²⁰ respectively). The effect of PTX volume on the S-LP distance did not vary with the chest level ($P = .746$), illustrated in Figure 6 by the parallel curves between the high and medium levels on both the right and left sides. With increasing PTX volumes, the lung point moved laterally and then medially with the subsequent withdrawal of air. Insufflation and deflation had the same absolute effect on the change in the S-LP distance ($P = .904$). The results of the mixed linear model analysis are summarized in Table 2.

DISCUSSION

Our study demonstrates that there is a linear relationship between PTX volume and the lateral position of the lung point during mechanical ventilation, and that ultrasound imaging is as accurate as CT imaging for localizing lung points. These findings are clinically relevant and may enable physicians to use ultrasonography to accurately follow the progression of PTXs during positive pressure ventilation.

Table 1—Difference in Lung Point Localization Between the Two Diagnostic Modalities Ultrasonography and CT Scanning

Measurements	Reader	No.	Mean, mm	SD, mm	Range, mm
Total	I	131	6.8	7.1	0.0-29.3
	II	131	8.1	7.5	0.0-29.4
Anterior chest	I	44	6.8	8.6	0.0-29.3
	II	38	7.1	7.8	0.0-27.2
Lateral chest	I	44	6.4	6.1	0.0-20.3
	II	45	8.6	8.2	0.0-28.5
Posterior chest	I	43	7.3	6.4	0.0-24.3
	II	48	8.4	6.6	0.0-29.4

Although it may seem reasonable to consider the size of the PTX when making procedural decisions, a newly published large prospective observational study found PTX size not to be an independent predictor of observation failure (defined as the subsequent need for a chest drain) in patients with blunt trauma. The most striking findings were that the patients whose occult PTXs expanded were > 70 times more likely to require chest tube drainage and that mechanical ventilation tripled this risk.²¹ This study used CXR imaging to assess the PTX progression, despite its being a poor method for detecting PTXs and one that underestimates the size.^{12,22} Two CT scan-based PTX classification systems, a linear size (thickness)-based algorithm^{23,24} and computer-aided volumetric measurements,²⁵ have been suggested as potential guides for making treatment decisions, but no consensus on the clinical usefulness of these PTX scoring systems has been established.²¹

The conceptual basis for using bedside thoracic ultrasound imaging in patients with occult PTX is that any PTX size progression should be detected early and treated promptly, without the need for patient transport or radiation exposure.^{26,27} There is little consensus on using lung point localization to grade PTX progression¹⁵ because the results in favor^{18,27} or opposed to using ultrasound imaging for this purpose^{14,28} are mixed. Blaivas et al¹⁴ argued that it is difficult to differentiate between medium- and large-sized PTXs, as evidenced by the weak correlation between increasing PTX volumes and the lateral position of the lung point on CT scans. They offered no statistical analysis or references to support this statement, only commenting on three CT images in the article. Soldati et al¹⁸ found a mean difference of 19 mm between ultrasound and CT scan lung points and they concluded that lung ultrasonography can be used to characterize PTX size and extension with an accuracy that approaches the reference standard. They excluded patients with occult PTX who needed mechanical ventilation because these patients often have more extensive and clinically significant PTXs. These assumptions may be invalid, because the occult PTX size and severity distributions in positive-pressure-ventilated patients are similar to nonintubated patients,⁵ and because clinically significant PTXs are equally frequent in both these patient groups.¹⁰

The remaining questions are whether an identifiable cohort of patients who are mechanically ventilated with occult PTX can be safely observed without undergoing tube thoracostomy,²⁹ and how these patients should be monitored. The first question remains controversial, pending completion of prospective randomized trials, whereas the second is addressed in this experimental study. Our results (a mean difference between the ultrasound and CT scan locations of only 6.8 mm)

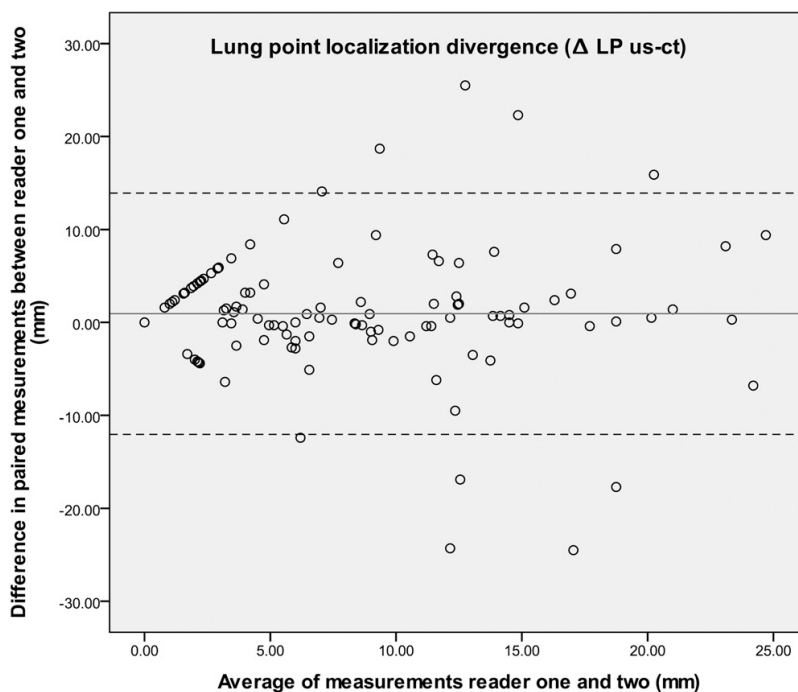


FIGURE 5. Bland-Altman plot of the paired measurements from the two readers. The high degree of agreement is indicated by a difference in measurements (the *y*-axis) that remains close to zero over the full measurement range (the *x*-axis). LP = lung point; us = ultrasound.

demonstrate that ultrasonography is comparable to CT imaging for localizing the lung point during positive pressure ventilation in a porcine model. The linear response of the S-LP distance to the PTX volume implies that the lung point moves in a progressive arc from the anterior to the lateral and to the posterior aspect of the chest wall as the PTXs expand. This progression was assessed at two different chest levels and was independent of whether the PTX was increasing or decreasing in size (Fig 6, Table 2).

Porcine anatomy is not identical to human anatomy, but the respiratory and cardiovascular systems are similar; therefore, pigs are an important animal model in biomedical research.^{30,31} Before commencing this study, we validated our PTX model using the reference standard CT scan and found equal distribution of intrapleural air as in supine patients with trauma.³² This study also revealed that the PTX volume and lung point position could easily be altered through insufflation and deflation. We performed all our measurements at the CT scan laboratory, which reduced the risk of any PTX progression occurring between the ultrasound and the CT scans. Soldati et al¹⁸ allowed up to 1 h to elapse between their tests, whereas all our measurements were performed during an inspiratory hold and within minutes of each other.

Unfortunately, the current study design, combined with the radiation hazard posed by serial CT scans, precludes using this experimental approach in human subjects.

We do recognize some limitations. First, one pig had a small amount of pleural fluid in the basal part of the right hemithorax that could have affected the localization of the lung point. Second, the thoracotomies may have introduced small amounts of air into the pleural cavities when the catheters were introduced, thereby increasing the actual PTX volume beyond the insufflated air volumes specified in the study protocol. Although excessive air was withdrawn using a 10-mL syringe before starting the air injections, it is possible that some air remained in the pleural cavity. This residual air may explain the differences in the mean S-LP distances of the right and left hemithoraces with equal PTX volumes (Fig 6). Another explanation for this finding may be the anatomic asymmetry of the thorax, with the presence of the heart in the left hemithorax affecting the air distribution. Finally, a large PTX can eliminate the lung point sign completely because the lung totally collapses and loses contact with the interior wall of the chest cavity. These patients often experience respiratory distress due to diminished lung capacity

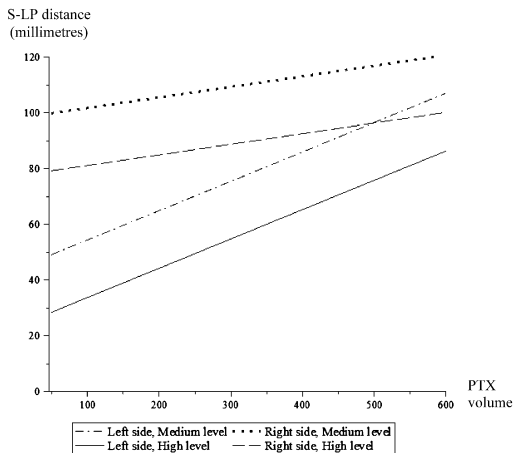


FIGURE 6. Graph illustrating the mixed linear model of the S-LP relative to the PTX volume. See Figure 2 and 4 legends for expansion of abbreviations.

and cardiovascular compromise due to tension PTXs.^{13,33} A tension PTX is diagnosed clinically and requires immediate needle decompression without the diagnostic delay associated with CXR or ultrasound imaging.¹

CONCLUSIONS

We have demonstrated that lung point movement is an indicator of PTX progression during positive pressure ventilation that can be evaluated as accurately by ultrasonography as by CT scanning. This

Table 2—Mixed Linear Model Analysis of the Sternum to Lung Point Distance Relative to the Pneumothorax Volume on the Thoracic Insufflation Side and Chest Level

Variable	Coefficient		F Test
	Estimate	95% CI	P Value
Intercept, mm	43.7	16.0 to 71.3	.010
Side ^a			
R	54.0	39.5 to 68.5	<.001
L	0.0	Reference	...
Level ^b			
High	-20.6	-27.7 to -13.4	<.001
Medium	0.0	Reference	...
Volume, mL	0.11	0.08 to 0.13	<.001
Thoracic side	-0.067	-0.11 to -0.03	.001
(R) × volume			
Thoracic side	0.000	Reference	...
(L) × volume			

L = left; R = right.

^aRight and left thoracic sides; the left is the reference.

^bChest level; high is between costae 2 and 3; medium is between costae 5 and 6 (reference).

finding may open up new possibilities for monitoring PTX development at the bedside. If a decision is made to observe patients who are mechanically ventilated with trauma and occult PTXs, we propose using serial thoracic ultrasound imaging to assess any PTX progression, which is known to be the strongest predictor of a patient's need for chest tube insertion. Further research should focus on the relationship between the cutaneous projections of the lung point and the optimal treatment options.

ACKNOWLEDGMENTS

Author contributions: Dr Oveland is the guarantor of the manuscript and takes responsibility for the integrity of the data and the accuracy of the data analysis.

Dr Oveland: contributed to the concept and design; analysis and interpretation of the data; acquisition of the ultrasound and CT imaging data; and the drafting, writing, review, revision, and approval of the manuscript.

Dr Lossius: contributed to the concept and design; analysis and interpretation of the data; and the writing, review, and approval of the manuscript.

Dr Wennelund: contributed to the concept and design, analysis and interpretation of the data, and review of the manuscript.

Dr Stokkeland: contributed to the concept and design, analysis and interpretation of the data, and review of the manuscript.

Dr Knudsen: contributed to the concept and design; analysis and interpretation of the data; acquisition of the ultrasound and CT imaging data; and the writing, review, revision, and approval of the manuscript.

Dr Sloth: contributed to the concept and design; analysis and interpretation of the data; acquisition of the ultrasound and CT imaging data; and the drafting, writing, review, and approval of the manuscript.

Financial/nonfinancial disclosures: The authors have reported to *CHEST* that no potential conflicts of interest exist with any companies/organizations whose products or services may be discussed in this article.

Other contributions: The authors acknowledge the Institute of Clinical Medicine, Aarhus University, and the Radiology Department, Aarhus University Hospital Skejby, for providing research facilities. Geir Egil Eide, PhD, statistician with the Western Norway Regional Health Authority, helped with the statistical computations. The study was performed at the Radiology Department, Aarhus University Hospital Skejby, Aarhus, Denmark.

REFERENCES

- Waydhas C, Sauerland S. Pre-hospital pleural decompression and chest tube placement after blunt trauma: a systematic review. *Resuscitation*. 2007;72(1):11-25.
- Karmy-Jones R, Jurkovich GJ. Blunt chest trauma. *Curr Probl Surg*. 2004;41(3):211-380.
- Neff MA, Monk JS Jr, Peters K, Nikhilesh A. Detection of occult pneumothoraces on abdominal computed tomographic scans in trauma patients. *J Trauma*. 2000;49(2):281-285.
- Trupka A, Waydhas C, Hallfeldt KK, Nast-Kolb D, Pfeifer KJ, Schweiberer L. Value of thoracic computed tomography in the first assessment of severely injured patients with blunt chest trauma: results of a prospective study. *J Trauma*. 1997;43(3):405-411.
- Ball CG, Kirkpatrick AW, Laupland KB, et al. Factors related to the failure of radiographic recognition of occult posttraumatic pneumothoraces. *Am J Surg*. 2005;189(5):541-546.
- Lamb AD, Qadan M, Gray AJ. Detection of occult pneumothoraces in the significantly injured adult with blunt trauma. *Eur J Emerg Med*. 2007;14(2):65-67.

7. Enderson BL, Abdalla R, Frame SB, Casey MT, Gould H, Maull KI. Tube thoracostomy for occult pneumothorax: a prospective randomized study of its use. *J Trauma*. 1993;35(5):726-729.
8. Tocino IM, Miller MH, Frederick PR, Bahr AL, Thomas F. CT detection of occult pneumothorax in head trauma. *AJR Am J Roentgenol*. 1984;143(5):987-990.
9. Brasel KJ, Stafford RE, Weigelt JA, Tenquist JE, Borgstrom DC. Treatment of occult pneumothoraces from blunt trauma. *J Trauma*. 1999;46(6):987-990.
10. Wilson H, Ellsmere J, Tallon J, Kirkpatrick A. Occult pneumothorax in the blunt trauma patient: tube thoracostomy or observation? *Injury*. 2009;40(9):928-931.
11. Ball CG, Lord J, Laupland KB, et al. Chest tube complications: how well are we training our residents? *Can J Surg*. 2007;50(6):450-458.
12. Ball CG, Hameed SM, Evans D, Kortbeek JB, Kirkpatrick AW; Canadian Trauma Trials Collaborative. Occult pneumothorax in the mechanically ventilated trauma patient. *Can J Surg*. 2003;46(5):373-379.
13. Barton ED. Tension pneumothorax. *Curr Opin Pulm Med*. 1999;5(4):269-274.
14. Blaivas M, Lyon M, Duggal S. A prospective comparison of supine chest radiography and bedside ultrasound for the diagnosis of traumatic pneumothorax. *Acad Emerg Med*. 2005;12(9):844-849.
15. Volpicelli G, Elbarbary M, Blaivas M, et al; International Liaison Committee on Lung Ultrasound (ILC-LUS) for International Consensus Conference on Lung Ultrasound (ICC-LUS). International evidence-based recommendations for point-of-care lung ultrasound. *Intensive Care Med*. 2012;38(4):577-591.
16. Committee for the Update of the Guide for the Care and Use of Laboratory Animals; National Research Council. *Guide for the Care and Use of Laboratory Animals*. 8th ed. Washington, DC: The National Academies Press; 2010.
17. Volpicelli G. Sonographic diagnosis of pneumothorax. *Intensive Care Med*. 2011;37(2):224-232.
18. Soldati G, Testa A, Sher S, Pignataro G, La Sala M, Silveri NG. Occult traumatic pneumothorax: diagnostic accuracy of lung ultrasonography in the emergency department. *Chest*. 2008;133(1):204-211.
19. Davis CS. *Statistical Methods for the Analysis of Repeated Measurements*. New York, NY: Springer; 2002.
20. Newcombe RG. Two-sided confidence intervals for the single proportion: comparison of seven methods. *Stat Med*. 1998;17(8):857-872.
21. Moore FO, Goslar PW, Coimbra R, et al. Blunt traumatic occult pneumothorax: is observation safe?—results of a prospective, AAST multicenter study. *J Trauma*. 2011;70(5):1019-1023.
22. Engdahl O, Toft T, Boe J. Chest radiograph—a poor method for determining the size of a pneumothorax. *Chest*. 1993;103(1):26-29.
23. Wolfman NT, Gilpin JW, Bechtold RE, Meredith JW, Ditesheim JA. Occult pneumothorax in patients with abdominal trauma: CT studies. *J Comput Assist Tomogr*. 1993;17(1):56-59.
24. de Moya MA, Seaver C, Spaniolas K, et al. Occult pneumothorax in trauma patients: development of an objective scoring system. *J Trauma*. 2007;63(1):13-17.
25. Cai W, Tabbara M, Takata N, et al. MDCT for automated detection and measurement of pneumothoraces in trauma patients. *AJR Am J Roentgenol*. 2009;192(3):830-836.
26. Lichtenstein DA, Mezière G, Lascols N, et al. Ultrasound diagnosis of occult pneumothorax. *Crit Care Med*. 2005;33(6):1231-1238.
27. Zhang M, Liu ZH, Yang JX, et al. Rapid detection of pneumothorax by ultrasonography in patients with multiple trauma. *Crit Care*. 2006;10(4):R112.
28. Sistrom CL, Reiheld CT, Gay SB, Wallace KK. Detection and estimation of the volume of pneumothorax using real-time sonography: efficacy determined by receiver operating characteristic analysis. *AJR Am J Roentgenol*. 1996;166(2):317-321.
29. Ball CG, Kirkpatrick AW, Feliciano DV. The occult pneumothorax: what have we learned? *Can J Surg*. 2009;52(5):E173-E179.
30. Rogers CS, Abraham WM, Brogden KA, et al. The porcine lung as a potential model for cystic fibrosis. *Am J Physiol Lung Cell Mol Physiol*. 2008;295(2):L240-L263.
31. Swindle MM, Smith AC, Hepburn BJ. Swine as models in experimental surgery. *J Invest Surg*. 1988;1(1):65-79.
32. Oveland NP, Sloth E, Andersen G, Lossius HM. A porcine pneumothorax model for teaching ultrasound diagnostics. *Acad Emerg Med*. 2012;19(5):586-592.
33. Barton ED, Rhee P, Hutton KC, Rosen P. The pathophysiology of tension pneumothorax in ventilated swine. *J Emerg Med*. 1997;15(2):147-153.